Vol.7 No.1 Jan 2024

Journal of Networking and Communication Systems

Received 2 November, Revised 20 December, Accepted 29 January

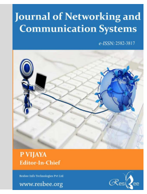

A CAD Tool for Enhanced Alzheimer's Detection using an Optimized Convolutional Neural Network with Amazon Cloud Space Training

Meher Nivedita Avdut
Grand Valley State University
Grand Rapids, Detroit, United States
mehernivedita.4@gmail.com

Abstract: Alzheimer's disease (AD) is a form of progressive irreversible dementia that occurs most frequently in older adults. It has been estimated that the number of patients who suffer from AD will double in the next two decades. Hence, early detection may help to clarify the mechanisms underlying AD and to improve the quality of life for AD patients. Thus, this paper intends to develop a novel Alzheimer's detection approach by following two phases namely, (a) pre-processing and (b) classification. Initially, the collected MRI is fed as input to pre-processing and filtering. The pre-processing of the image is accomplished here using and Contrast-Limited Adaptive Histogram Equalization (CLAHE) and filtering via Gaussian blur, median blur, bilateral blur. Then, the filtered MRI image is subjected to classification using optimized CNN. The outcomes from CNN exhibit the presence or absence of the disease. As a novelty, the weight of optimized CNN is regularized using a new optimization referred to as the Scrounger Customized Rider Optimization Algorithm (SC-ROA), which is the hybridization of the standard Rider Optimization Algorithm (RAO) and Group Search Algorithm (GSO). These regularized weights are optimized further with the Genetic Algorithm (GA) and ADAM optimizer. The outcomes from GA are the optimized weights. The performance of the proposed model is analyzed in terms of both positive and negative measures.

Keywords: Alzheimer's Disease; CLAHE; Filtering; Optimized CNN; SC-ROA.

Nomenclature

Abbreviation	Description
SGD	Stochastic Gradient Descent
MCI	Mild Cognitive Impairment
SPECT	Single Photon Emission Computed Tomography
ROI	Regions Of Interest
FDG-PET	Fluoro Deoxy Glucose Positron Emission Tomography
PET	Positron Emission Tomography
MRI	Magnetic Resonance Images
PSO	Particle Swarm Optimization
AD	Alzheimer's Disease
RNN	Recurrent Neural Networks
CNN	Convolutional Neural Networks
SPM	Statistical Parametric Mapping
BGRU	Bidirectional Gated Recurrent Units
CAD	Computer-Aided Diagnosis
GM	Gray Matter
NMF	Nonnegative Matrix Factorization
MCC	Maximum Clique Centrality
CLAHE	Contrast-Limited Adaptive Histogram Equalization
SC-ROA	Scrounger Customized Rider Optimization Algorithm
ROA	Rider Optimization Algorithm
GSO	Group Search Algorithm
VBC	Voxel-Based Classifier
FPR	False Positive Rate
FNR	False Negative Rate
FDR	False Discovery Rate
MM-SDPN	Multi Modal Stacked DPN
CBIR	Content-Based Image Retrieval
HCs	Healthy Controls
SVM	Support Vector Machine
3D-CapsNets	3D-Capsule Networks
CluViaN	Clustering Via Network
CDF	Cumulative Distribution Function
ADNI	Alzheimer's Disease Neuro imaging Initiative
TP	Training Percentage

https://doi.org/10.46253/jnacs.v7i2.a4

1. Introduction

In recent days, the most common mental disorder in all ages of people is Alzheimer's disease and this is the root cause for dementia [9] [10]. In general, a neurodegenerative disease of the brain that causes severe damage to the brain function, affecting the neurons and brain cells is referred to the Alzheimer's disease. This disease takes the human to serious unrecoverable stages like memory impairment, changes in behavior, and thinking, and no longer makes the brain function normally [11] [24]. The disease initially affects the brain and makes the recent events to be lost. It further keeps on progressing and leads to long-term memory loss. It also spreads to different areas of the brain and affects the functions or the specific abilities of the concerned area like judgment, attention, language, etc.

Over time, the disease gets worse and does not even enable a person to carry out basic body functions like walking and swallowing [12] [13]. The Plaques, Loss of nerve cell connections, and Tangles are the hallmarks of Alzheimer's disease process. The healthy brain cell is damaged in the Plaques and tangles, which further die out and make the brain shrink leading to confusion, memory loss, mood swings, and speech problems [14]. In the disease progression, there are four different stages, MCI, Mild AD, Moderate AD, and Severe AD [20] [21]. MCI does not alter daily life significantly and Mild, as well as Moderate AD, are characterized by enhancement in the cognitive deficits. However, the Severe AD diminishes the independence of patients.

The diagnosis of Alzheimer's disease by image pre-processing is a primary step to screen the progression of the disease and here the alterations in the brain are assessed accurately by Neuro imaging techniques. Understanding the brain of Alzheimer's patients is of great clinical importance [22] [23]. The early detection of the disease by functional imaging modalities like SPECT and PET are efficient in making reliable decisions. On the other hand, before irreversible damage in the brain, Alzheimer's disease can be detected with MRI [15] [16]. The 3D map models on the rate of glucose consumption of the brain are analyzed by PET, which is referred to non-invasive medical imaging modality [25]. With the medical imaging technique, there is a requirement for manual intervention for screening the boundaries and the affected areas. So, the detection of Alzheimer's disease continued with the automated diagnosis for accurate detection [17].

The most commonly used Alzheimer's detection technique is K-NN as it is simple and has low design complexity [33]. The major drawback of this model lies in the requirement for large memory and the larger recognition time. Further, PCA is an efficient technique that works well in reducing the correlation between image components and makes the image be viewed clearly. However, this method has rejected the high-order correlation value and reduced the classification accuracy [19]. Further, to have a better prediction performance for Alzheimer's, it is necessary to construct a simple yet efficient method.

The major contribution of this research work is:

- The preprocessing of the input image is carried out with CLAHE and filtered using Gaussian blur, median blur, and bilateral blur filters.
- For classification, a new optimized CNN is introduced in this work, where the weights are optimally tuned by a new hybrid algorithm.
- A new optimization referred to Scrounger Customized Rider Optimization Algorithm (SC-ROA) is introduced in this work, which is the hybridized form of ROA and GSO.

The rest of the paper is organized as section 2 provides a compact review of the works undergone in the literature concerning the subject. Section 3 tells about the proposed convolutional neural network-based Alzheimer's disease prediction model. Section 4 portrays image pre-processing: CLAHE and filtering process. In addition, Section 5 describes the classification via optimized CNN: proposed hybrid optimization on finding optimal weight. Finally, the results acquired are discussed in Section 6 and a strong conclusion to this research is given in Section 7.

2. Literature Review

1.1 Related Works

In 2016, Rahim *et al*. [1] have proposed VBC for the detection of Alzheimer's disease with the aid of the connectivity-metabolism relationship and here the region-to-voxel connectivities were evaluated using huge ROIs. The 3D-based FDG-PET images at the voxel level were classified using a linear classifier. The features of the image were obtained by utilizing the computing region-to-voxel connectivity maps. From the functional atlas, the Seed-based correlations were computed with the extracted ROIs.

In 2018, Shi *et al*. [2] have formulated an MM-SDPN algorithm embedded with two-stage SDPN to fuse multimodal data for accurate detection of Alzheimer's disease from multimodal neuroimaging datasets. The high–level features from both MRI as well as PET were learned using two SDPNs. The extracted features were fed as input to the SDPN to link the multimodal neuroimaging information.

In 2019, Kruthika *et al*. [3] have proposed a technique for Alzheimer's Disease detection with a multistage classifier by particle swarm intelligence-based feature selection technique. The input image from MRI was pre-processed using Free Surfer, which follows the steps like head motion correction, smoothing, compensation for slice-dependent time shift, and normalizing. The pre-processed image was subjected to extract the features and optimal features from the image were selected using PSO. The extracted optimal features were classified using several classifiers like KNN, SVM, MLP, and the ensemble model.

In 2019, Cui *et al*. [4] have projected an innovative AD diagnosis model using integrating the spatial and longitudinal features of MR images with the help of CNN as well as RNN. For the classification task, the spatial features of MRI were learned by constructing CNN, and the longitudinal features were extracted at multiple time points with the help of BGRU connected at the output of CNN. The proposed model was evaluated in terms of classification accuracy, specificity, sensitivity, and area under the receiver operating characteristic curve (AUC) with the ADNI dataset.

In 209, Kruthika *et al*. [5] have projected a CBIR system to detect Alzheimer's in an early stage with a 3D-Convolutional Neural Network, 3D Capsule Network, and pre-trained 3D-autoencoder technology. The image acquired from the MRI was preprocessed by utilizing the software- SPM. For the smaller dataset, the 3D-CapsNets were efficient in handling robust image transitions and rotations. The detection performance of the model was enhanced using 3D-CapsNets when compared to CNN.

In 2017, Beheshti *et al.* [6] have formulated an innovative CAD system with the aid of a genetic algorithm as well as feature ranking for analyzing structural magnetic resonance images. Initially, the global and local GM were investigated by comparing them with HCs via a voxel-based morphometry technique. Then, the features were ranked in the feature selection stage based on t-test scores. Then, the optimal feature set was selected using the genetic algorithm. The optimal features were subjected to classification using SVM.

In 2018, Liu *et al*. [7] have introduced an unsupervised clustering method using NMF to detect AD. The consensus clustering matrix was utilized for the factorizations of different views. The incomplete data problem was solved by weight matrices. The model was evaluated using AD datasets and the outcomes of the evaluations were noted. The results revealed an enhancement in the performance of the proposed model over the existing one in terms of clustering accuracy and convergence speed.

In 2018, Manners *et al*. [8] have proposed CluViaN to identify the genes that were responsible for Alzheimer's disease and this detection has accomplished the analyzing modules of co-expression networks. The ranking of the influential genes was extracted from central genes inside functional modules and they were ranked based on MCC scores.

1.2 Review

Table 1 portrays the different research work accomplished to detect Alzheimer’s disease. It also provides a clear explanation of the features as well as the challenges faced by each of the models. In further research works, there is a necessity to generate a novel technique that will overcome these drawbacks. VBC has high classification accuracy and the modality of imaging is enhanced. However, it is unable to tackle the connectivity of high dimensionality of voxel and it too requires dimensionality techniques in the clustering approach to reduce the dimensionality of the image and to enhance the accuracy further [1]. A lower computational complexity is achieved with MM-SDPN and it suffers the drawback of over fitting [2]. With PSO [3], the retrieval speed is high and it is complex to select effective biomarkers. Then, CNN and RNN have higher sensitivity as well as specificity. But, the major shortcomings of these models is, that the irrelevant information was not completely discarded [4]. A higher classification accuracy and higher retrieval accuracy are achieved with a two-fold CNN and Caps Net model [5]. But, the major disadvantage of this model lies in the large data sets required for training. The SVM-based classification model was efficient in extracting complex spatial patterns and the specificity is also high. Apart from this advantage, there is a huge shortcoming with sensitivity and classification accuracy [6]. NMF Solves the issue related to incomplete data problems and this model suffers from limited feature space and improper feature selection techniques [7]. In the biological network, the problem of overlapping was avoided and this model is insufficient for co-expression networks.

Table 1: *Features and challenges of State-of-the-art Alzheimer's disease detection*

Author Citation	Methodology	Features	Challenges
Rahim *et al.* [1]	VBC	✓ High classification accuracy. ✓ Imaging modality is enhanced.	× Unable to tackle the connectivity of high dimensionality of voxel. × Requires dimensionality reduction in clustering models.
Shi et al. [2]	MM-SDPN	✓ Low computational complexity.	× Suffers from the problem of overfitting.
Kruthika et al. [3]	PSO	✓ Retrieval speed is high	× The selection of effective biomarkers was complex.
Cui *et al.* [4]	CNN and RNN	✓ High sensitivity and specificity	× Irrelevant information was not completely discarded.
Kruthika *et al.* [5]	CNN and CapsNet	✓ High F1-score ✓ Higher retrieval accuracy.	× Requires large data sets for training.
Beheshti *et al.* [6]	SVM	✓ High specificity ✓ Efficient in extracting complex spatial patterns.	× Low classification accuracy × Low sensitivity
Liu *et al.* [7]	NMF	✓ Solves the issue related to incomplete. ✓ Data problem ✓ High convergence speed	× Optimal features were not selected optimally. × Limited feature space
Manners et al. [8]	CluViaN	✓ Detected intrinsic modules as well as overlapping in the biological networks.	× Insufficient co-expression networks

3. Proposed Convolutional Neural Network-based Alzheimer's Disease Prediction Model

3.1 Proposed Archi Type

The proposed Alzheimer's detection approach encloses two phases namely, (a) Pre-processing and (b) Classification. Initially, the collected MRI images(Im_{in})(in HDR form) are fed as input to pre-processing phases, in which the pre-processing is accomplished using and CLAHE and filtering like Gaussian blur, median blur, bilateral blur.Then, the pre-processed MRI image(Im_{pre}) is subjected to classification via optimized CNN. The outcomes of CNN(Im_{out})portray, whether the MRI image is diseased or non-diseased. In general, a network with massive weight is a sign of unstableness and here a smaller change in input might cause a larger change in output. This is due to the over fitting of the training dataset. Weight regularization is the optimal solution for this scenario. A new logic is introduced in this aspect that finds the regularized weight using optimization algorithms. For this, a new hybrid algorithm (SC-ROA) that evaluates the new weight updating formulation is introduced in this work and subsequently, the GA and ADAM optimizer plays a major role in producing the final optimal weight. Moreover, the training of CNN will be carried out using Amazon cloud space to reduce the computational complexity. Fig. 1 depicts the architecture of the proposed Alzheimer's detection model. The pseudo-code of the proposed work is shown in Algorithm 1.

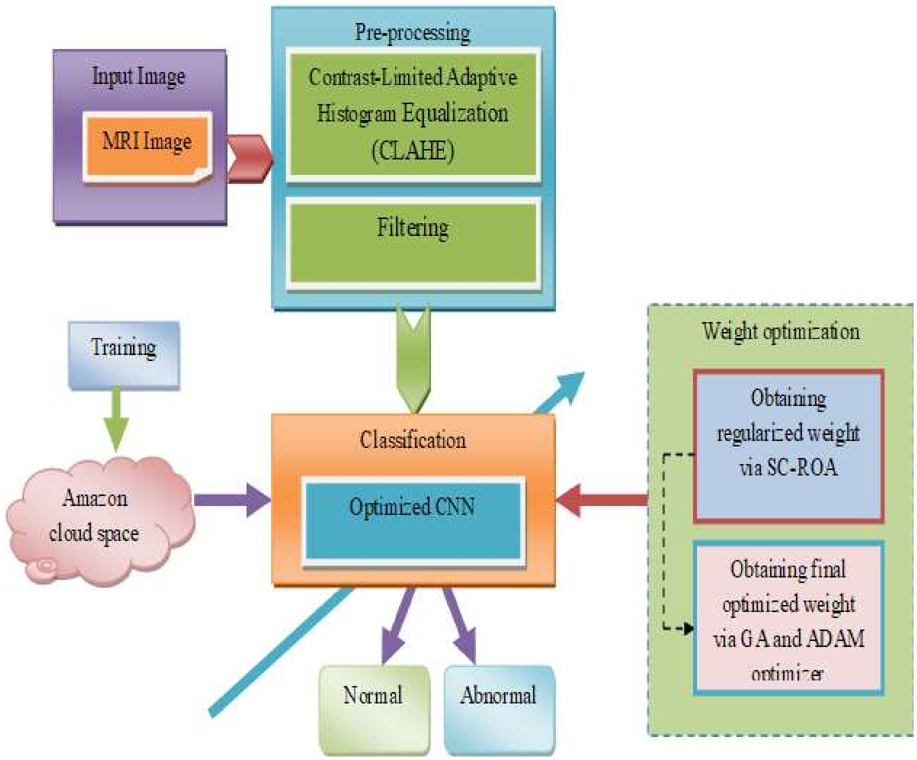

Fig. 1. *Block diagram of the proposed Alzheimer's detection framework*

Algorithm 1: Steps involved in proposed Alzheimer's disease prediction model	
Steps	Procedure
Step 1	Initially, the data collected from patient EHR is pre-processed
Step 2	The pre-processed outcomes are fed as input to CNN and the resultant is the benign (generally harmless) or malignant (cancerous) growths
Step 3	As a novelty, the weight optimization (wi) in CNN is undergone by means of regularizing the overall weights, so as to acquire more precious results
Step 4	The overall weight $(wi_1, wi_2, ..., wi_n)$ is fed as input to the proposed hybrid optimization algorithm SC-ROA. The regularized weights $(r.wi_1, r.wi_2, ..., r.wi_n)$ are the results from the proposed hybrid optimization algorithm.
Step 5	Subsequently, the regularized weights (2nd solution in solution encoding) are fed as input to GA.
Step 6	The outcome from GA and ADAM optimizer is the optimized weight $(o.wi_1, o.wi_2, ..., o..wi_n)$ that is acquired by resolving the objective function, (i.e., error minimization $E(r)$ (inverse of accuracy) between actual and predicted outcomes) as per Eq. (1). $$\min(E(r)) = Actual - \Pr edicted \quad (1)$$

4. Image Pre-processing: CLAHE and Filtering process

4.1pre-Processing

It is the initial stage of analysis and it helps to enhance the quality of the image that is being processed. The input MRI image (Im_{in}) is subjected to pre-processing, in which the following process takes place:

(a) Read the image: Here, the path of the MRI image dataset is stored in a variable ($temp$).

The input MRI image (Im_{in}) is read using the function expressed in Eq. (2)

$$\mathrm{Im}_{in} = temp.get - fdate() \quad (2)$$

(b) Normalize the image: The image is sliced and normalized within the range 0 to 255. It is accomplished with the function expressed in Eq. (3). The normalized image is denoted as Im_{nor}

$centre-slice1 = centre-slice / centre-slice\max()$ (3)// for 1st slice

(c) Filtering: The normalized image (Im_{nor}) is filtered using four different filters:

***Gaussian Blur (Gaussian smoothing)*:** It is a type of Gaussian filter that blurs an image using a Gaussian function. In 1-D space and 2-D space, the Gaussian functions are mathematically expressed in Eq. (4) and Eq. (5) respectively. Here, x is the distance from the origin in the horizontal axis and y is the distance from the origin in the vertical axis. In addition, the Gaussian distribution's standard deviation is denoted as σ. The Gaussian filtered image is denoted as Im_{Ga}.

$$G(x) = \frac{1}{\sqrt{2\Pi\sigma^2}} e - \frac{x^2}{2\sigma^2} \tag{4}$$

$$G(x, y) = \frac{1}{\sqrt{2\Pi\sigma^2}} e - \frac{x^2 - y^2}{2\sigma^2} \tag{5}$$

(ii)Median Blur: It is a non-linear digital filtering approach utilized to remove the noise from the normalized image (Im_{nor}). In digital image processing, median filtering is deployed to preserve the edges of the normalized image (Im_{nor}), while removing the noise. The median filtered image is denoted as Im_{med}.

(iii) Bi-lateral Blur: A bilateral filter is a non-linear, edge-preserving, and noise-reducing smoothing filter for images. This bi-lateral filter replaces each pixel intensity with a weighted intensity of average values from neighboring pixels. Mathematically, the bilateral filter is expressed in Eq. (6).

$$\mathrm{Im}^{filter}(x) = \frac{1}{Wt_p} \sum_{x_i \in \Omega} \mathrm{Im}_{norm}(x(i)).F_r\left(\left\|\mathrm{Im}_{norm}(x(i)) - \mathrm{Im}_{norm}\right\|\right) \\ g_s\left(\left\|(x((i)) - (x)\right\|\right) \tag{6}$$

Here, Wt_p is the assigned weight, Im^{filter} is the filtered image, x is the coordinate of the current pixel to be filtered, F_r is the kernel range for smoothing the intensity difference. In addition, g_s is the spatial kernel for smoothing the coordinate difference in the image. The weight Wt_p is mathematically expressed in Eq. (7). The bi-lateral filtered image is denoted as Im_{Bi}.

$$Wt_p = F_r\left(\left\|\mathrm{Im}_{norm}(x(i)) - \mathrm{Im}_{norm}\right\|\right) g_s\left(\left\|(x((i)) - (x)\right\|\right) \tag{7}$$

(iv) CLAHE: There are five major procedures in the CLAHE pipeline. Initially, the normalized image (Im_{nor}) is portioned into equal-sized rectangular blocks, and then to each of the rectangular boxes, the histogram adjustments like the creation of histogram, clipping, and redistribution are performed. Moreover, from the clipped histogram, the CDF provides the mapping function. In between the rectangular boxes, the bilinear interpolation is accomplished to reject the possible block artifacts. In each block, the clip point (α) helps enhance the contrast, and it is exhibited mathematically in Eq. (8). The count of pixels and the dynamic range in each rectangular box are represented using the terms J and K respectively. The maximum slope and clip factor are symbolized as Max_{slope} and β respectively.

$$\alpha = \frac{J}{K}\left(1 + \frac{\beta}{100} Max_{slope}\right) \tag{8}$$

Resize the Image: To visualize the modifications, the image resizing takes place in CLAHE. The resized image is denoted as $\mathrm{Im}_{re-size}$. The resized image of the Gaussian, median, and bi-lateral filter is defined in Eq. (9), Eq. (10), and Eq. (11) respectively. The overall re-sized image $\mathrm{Im}_{re-size}$ is acquired as given in Eq. (12).

$$\mathrm{Im}_{re-size}(Ga) = Clahe - filter(\mathrm{Im}_{Ga}) \text{ //Gaussian filter} \tag{9}$$

$$\mathrm{Im}_{re-size}(Med) = Clahe - filter(\mathrm{Im}_{med}) \text{ //Median filter} \tag{10}$$

$$\mathrm{Im}_{re-size}(Bi) = Clahe - filter(\mathrm{Im}_{Bi}) \text{ //Bi-lateral filter} \tag{11}$$

$$\mathrm{Im}_{re-size} = \mathrm{Im}_{re-size}(Ga) + \mathrm{Im}_{re-size}(Med) + \mathrm{Im}_{re-size}(Bi) \tag{12}$$

The re-sized image is subjected to classification via optimized CNN.

5. Classification via optimized CNN: Proposed hybrid optimization on finding Optimal Weight

5.1 Optimized CNN

CNN is a famous deep learning architecture with three layers: fully connected, pooling, and convolution (multiple hidden layers). The learning of the input features takes place in the convolutional layer. The convolutional layer encompasses diverse convolution kernels that aid in computing different feature maps. With the aid of diverse kernels, the overall feature map is acquired. The location (x, y) of the n^{th} feature map corresponding to q^{th} the layer is $M^{q}_{x,y,z}$. This can be expressed mathematically in Eq. (13). The notation wi^{q}_{n} is the weight vector of q^{th} layer regarding n^{th} filter. In addition, bi^{q}_{n} is the bias term.

$$M^{q}_{x,y,z} = wi^{qT}_{n} g^{q}_{x,y} + bi^{q}_{n} \tag{13}$$

At the location (x, y), the input patches localized at n^{th} layer is $g^{q}_{x,y}$. The non-linear features are detected in the multi-layer networks by means of introducing the activation function. In the convolutional features $M^{q}_{x,y,z}$, the activation function $\left(act^{q}_{x,y,z}\right)$ is computed by using Eq. (14).

$$act^{q}_{x,y,z} = act\left(M^{q}_{x,y,z}\right) \tag{14}$$

The resultants of the convolutional layer enter the pooling layer, where the shift-variance is achieved using lessening the resolution of the feature maps. The pooling function is denoted as $pool(\ )$ and around the location (x, y), and the local neighborhood for each feature map $\left(act^{q}_{t,v,n}\right)$ is represented as $Rn_{x,y}$, which is expressed in Eq. (15).

$$yi^{q}_{x,y,x} = pool\left(act^{q}_{t,v,n}\right), \forall (t,v) \in Rn_{xy} \tag{15}$$

The final layer of CNN is the output layer. Then, for each of the specific tasks, the optimum parameters are acquired using minimizing the suitable loss function $(Loss)$ corresponding to the task. Mathematically, the loss function $(Loss)$ is determined using Eq. (16).

$$Loss = \frac{1}{R}\sum_{n=1}^{R} q\left(\theta; yi^{(n)}, oi^{(n)}\right) \tag{16}$$

Here, all the parameters of CNN (θ) corresponding to input-output desired R relations are as $\left\{\left(xi^{(n)}, yi^{(n)}\right); n \in [1, \cdots, R]\right\}$. The n^{th} input data, the corresponding target labels, and the output of CNN are represented as $xi^{(n)}$, $yi^{(n)}$ and $oi^{(n)}$ respectively.

5.2 Proposed Hybrid SC-ROA for Weight Optimization

The standard ROA [26] was based on the group of riders, who are moving towards the goal to be a runner of the race. ROA encloses four major groups of riders, namely bypass rider, follower, overtaker, and attacker. This optimization algorithm is good at solving complex issues but it requires some improvement due to its slower convergence. On the other hand, GSO [27] is based on animal searching behavior. It solves large-scale optimization problems with three kinds of members namely producers, scroungers, and rangers. The standard GSO gets trapped into local optimal solutions and hence requires improvement. Thus, the standard GSO and ROA are hybridized here to form a new optimization algorithm referred to as SC-ROA. In literature, more than optimization principles or mechanisms have been combined to develop a hybrid optimization algorithm [32]. A new update evaluation is introduced to make the update of weight in CNN. The procedure of the proposed algorithm is as follows:

(a) Initialization: This is the initial stage and here the search agents of both GSO and ROA are initialized. Since, in the new update procedure, the over taker of ROA and scrounger of GSO is utilized as a key to solving the optimization problem, they are alone initialized.

Over taker of ROA: In general, The over taker tries to reach the target by overtaking theleading rider. The over taker is denoted as OR.

***Scrounger of GSO*:** Towards the producer, the scrounger makes a random walk to reject the local minima.The scrounger is denoted as Sc.

(b)Success rate evaluation: The success rate is determined between the location of the rider and the target. The success rate is computed for every iteration and the positional update of the search agent is based on this success rate.

(b) Elaborating Over taker and Scrounger Update

***(i) Over taker update of ROA*:** The position of the over taker in the direction indicator d^{t} at a time t is indicated using the term X^{t}. In this proposed strategy, the new overtaker update evaluation is expressed in Eq. (17).

$$X^{t+1}_{OR} = X^{t} + \left[d^{t} + X^{t}_{\mathrm{Reg}}\right] \tag{17}$$

The distance traveled by the over taker is represented using the term d^{t} and it is the multiple of the velocity of r^{th} the rider and the off time, which is mathematically shown in Eq. (18).

$$d_r^{tm} = \left[\frac{2}{1-\log\left(S_R^t\right)}\right] - 1 \tag{18}$$

The newly derived formula for the relative success rate $\left(S_R^t(r)\right)$ of r^{th} riderat the time t is computed mathematically as per Eq. (19). This modified form of relative success rate $\left(S_R^t(r)\right)$ is suitable for the minimization function. Here, q_t is the regularization function and $\min_{r=1}^{N}$ is the min (regularized weights).

$$S_R^t(r) = 1 - \frac{\min_{r=1}^{N} q_r^t}{q_t} \tag{19}$$

(ii) *Scrounger update of GSO*: "During each searching bout, some group members are selected as scroungers" The area copying the behavior of the scrounger is modeled toward the producer in the form of a random walk. This is expressed in Eq. (20). The uniform random sequence is denoted as k .

$$X_{Sc}^{t+1} = X^t + k_3 \times \left(X^{reg} - X^t\right) \tag{20}$$

Proposed hybrid update evaluation: As mentioned earlier, both the update formulas of over taker and scrounger are combined to introduce the new hybrid formulation. The derivation is as follows:

$$X^{t+1} = \frac{1}{2}\left(X_{OR}^{t+1} + X_{Sc}^{t+1}\right) \tag{21}$$

$$X^{t+1} = \frac{X^t + \left[d^t * X_{\mathrm{Re}g}^t\right] + X^t + k_{1\times N} \times \left(X^{reg} - X^t\right)}{2} \tag{22}$$

$$X^{t+1} = X^t + \frac{d^t}{2} + \frac{X_{\mathrm{Re}g}^t}{2} + \frac{X^t}{2} + \frac{k_3 X^{reg}}{2} - \frac{k_3 X^t}{2} \tag{23}$$

$$X^{t+1} = X^t + X_{\mathrm{Re}g}^t\left(1 + \frac{k_3}{2}\right) - \frac{k_3 X^t}{2} + \frac{d^t}{2} \tag{24}$$

$$X^{t+1} = X^t\left(1 - \frac{k_3}{2}\right) + X_{\mathrm{Re}g}^t\left(1 + \frac{k_3}{2}\right) + \frac{d^t}{2} \tag{25}$$

The final update expression for the search agent is expressed in Eq. (25).

$$X^{t+1} = \left(X^t + X_{\mathrm{Re}g}^t\right)k_3 + \frac{d^t}{2} \tag{26}$$

$$X^t = \begin{cases} 1; & if\, X^{t+1} > 15 \\ 0; & else \end{cases} \tag{27}$$

$$X_{\mathrm{Re}g}^t = \arg \min_{X^t = 1,2,\ldots,present\, iteration} \sum\left(X^t\right)^2 \tag{28}$$

The new expression d^t is shown in Eq. (29). Here, C_k is a constant and its value is 100. The modified form of the relative success rate $\left(S_R^t(r)\right)$ is expressed in Eq. (30).

$$d^t = \left[\frac{2}{1-\log\left(S_R^t\right) + C_k}\right] - 1$$

$$S_R^t(r) = 1 - \frac{rank\left(X_{\mathrm{Re}g}^t\right)(==1)}{rank\left(X^t\right)} \tag{29}$$

$$\text{So, } S_R^t(r) = 1 - \frac{1}{rank\left(X^t\right)} \tag{30}$$

The outcomes from the hybridized process are the regularized weights $\left(r.wi_1, r.wi_2, \ldots, r.wi_n\right)$, which are fed as input to the traditional GA. Typically, GA is a heuristic search and optimization technique that was constructed based on the motivation acquired from the natural evolution process. This algorithm is being employed for a huge count of real-world problems to diminish the complexity. In the current research work, the GA-based ADAM optimizer is utilized to achieve the optimized result (final optimal weight).

5.3 Solution Encoding and Objective Function

Two solutions are fed as input in two different stages. During, the weight regularization, the overall weight $(wi_1, wi_2, ..., wi_n)$ of the network is fed as input to the proposed SC-ROA model. The regularized weights $(r.wi_1, r.wi_2, ..., r.wi_n)$ are the outcomes from the proposed SC-ROA model. This is said to be the 1st solution, which is diagrammatically represented in Fig. 2. Subsequently, the regularized weights $(r.wi_1, r.wi_2, ..., r.wi_n)$ are fed as input to GA. The optimized weighted output is the outcome from GA and it is said to be the 2nd solution in solution encoding. A diagrammatic representation of this is illustrated in Fig. 3. The major objective of this research work is to enhance the detection accuracy, and the objective function Obj is mathematically expressed in Eq. (31).

$$Obj = \max imization(accuracy) \tag{31}$$

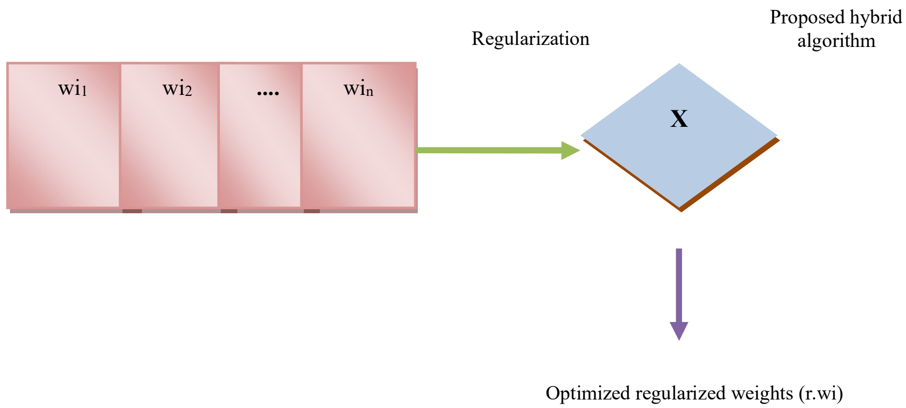

Fig. 2. *Solution Encoding (weight regularization)*

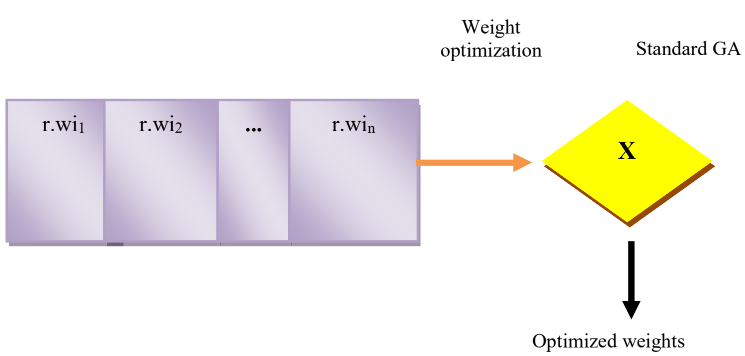

Fig. 3. *Solution Encoding (optimized weights)*

The pseudo-code of the proposed SC-ROA model is shown in Algorithm 2. The flow of the proposed model is exhibited in Fig. 4.

Algorithm 2: Pseudo-code of Sc-ROA approach	
Step 1	Population initialization
Step 2	Initialize t
Step 3	If $(t > \max(t))$
	then
Step 4	Proposed update evaluation
	The new over taker update of ROA is accomplished using Eq. (17)
	The scrounger update of GSO is achieved using Eq. (20)
	The final update of the search agent is achieved using Eq. (25)
Step 5	Proposed success rate evaluation
	The relative success rate $\left(S_R^t(r)\right)$ is computed using Eq. (30)
	Else
Step 6	Terminate

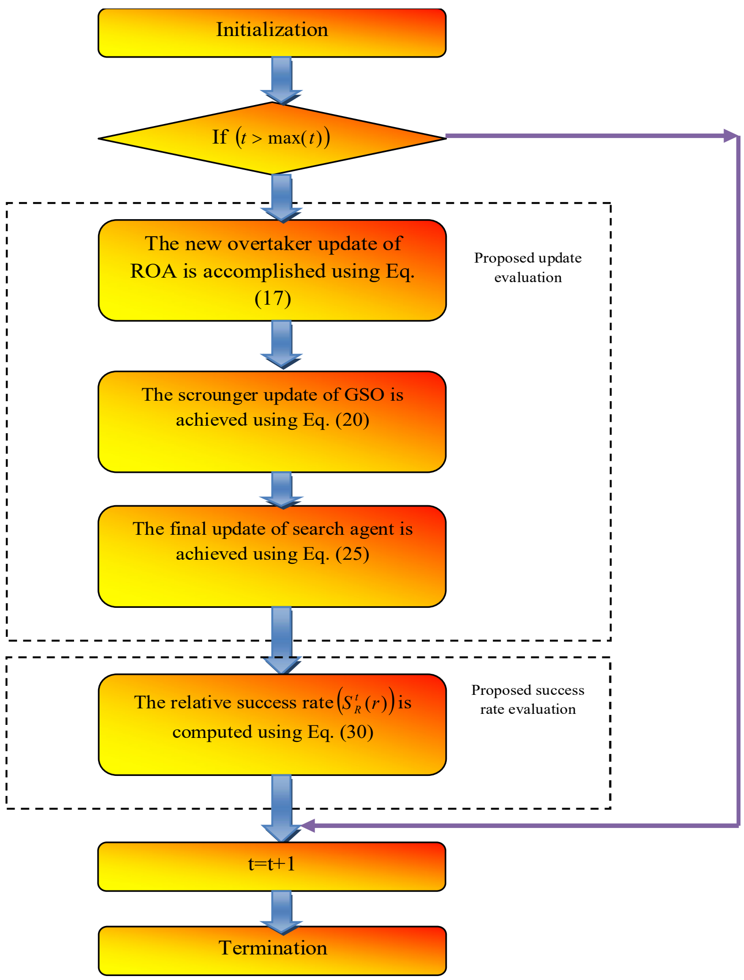

Fig. 4. *Flow chart of the proposed SC-ROA model*

6. Results and Discussions

6.1 Experimental Setup

The proposed Enhanced Alzheimer's Detection using Optimized DCNN was implemented in PYTHON and the corresponding resultants acquired are noted. "The data used in the preparation of this article were obtained from the ADNI database adni.loni.usc.edu. The ADNI was launched in 2003 as a public-private partnership, led by Principal Investigator Michael W. Weiner, MD. The primary goal of ADNI has been to test whether serial MRI, PET, and other biological markers, together with clinical and neuropsychological assessment, can be combined to measure the progression of MCI and early

Alzheimer's disease (AD). For up-to-date information, see www.adni-info.org [1]".This evaluation is undergone for the presented work over the traditional works in terms of both positive and negative measures. The accuracy, sensitivity, specificity, and precision fall under the positive measures, while FNR, FDR, FPR, and FOR are the negative measures. All these evaluations are undergone using varying the TP. The performance of the presented work (SC-ROA+GA+ADAM) is compared over the extant optimizers like SGD [28], ADAGRAD [29], RMSPROP [30], and ADAM [31]. Further, the performance evaluation of the presented work (proposed CNN with SC-ROA) is evaluated by varying the learning percentage.

6.2 Performance Evaluation of the Presented Work (Proposed CNN with SC-ROA): by Varying TP's

The presented work is evaluated in terms of both positive and negative measures for revealing its betterment over the varying TP's. The performance of the presented model (Proposed CNN with SC-ROA) is evaluated by varying the TP's and the resultant is shown in Fig.6, Fig. 7, Fig. 8, and Fig. 9 for TP=50, TP=60, TP=70, and TP=80, respectively. The accuracy of the presented work at TP=50, TP=60, TP=70, and TP=80 is (~)0.87, (~)0.936, (~)0.941, and (~)0.9370, respectively. Thus, from the evaluation, it is obvious that the accuracy of the presented works is higher at TP=70 and lower than TP=50. Further, for the highest accuracy of the presented work (i.e. at TP=70), the presented work is 6.9%, 0.56%, and 0.5% better than the presented work at TP=50, TP=60, and TP=80, respectively. On the other hand, the resultants of the sensitivity of the presented work are shown in Fig. 6 (b). The sensitivity of the presented work at TP=50 is (~)0.9370, TP=60 is (~)0.973, TP=70 is (~)0.966 and TP=80 is (~)0.988. Here, the highest sensitivity is recorded by the presented work at TP=80 and it is 4.7%, 1.47%, and 2.1% better than the sensitivities of the present work at TP=50, TP=60, and TP=70, respectively. Thus, from the evaluation, it is obvious that the presented work is more accurate for higher TP's. Further, the FPR (negative measure) of the presented work records the lowest value at TP=80, and it is 79%, 55%, and 64.5% better than the FPR of the presented works at TP=50, TP=60, and TP=70, respectively. As a whole, it is clear that the presented work is more significant for higher TP's.

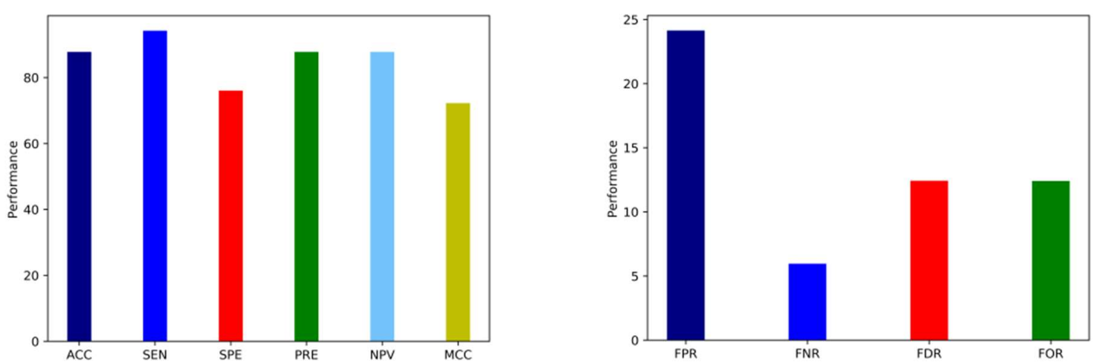

(a) (b)

Fig. 5. *Performance Evaluation of the presented work for varying 50% of TP for (a) Positive and (b) Negative measures*

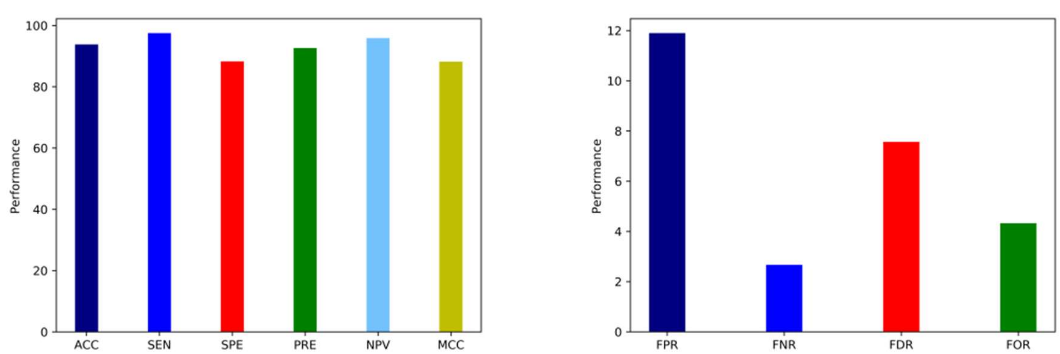

(a) (b)

Fig. 6. *Performance Evaluation of the presented work for varying 60% of TP for (a) Positive and (b) Negative measures*

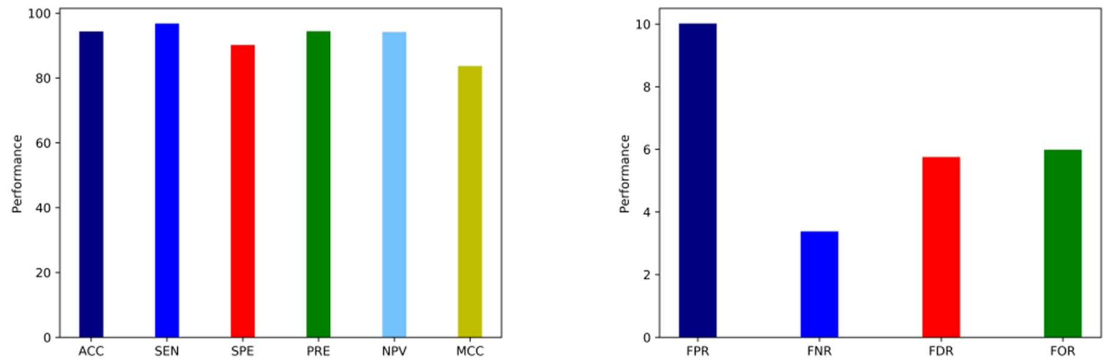

(a) (b)

Fig. 7. *Performance Evaluation of the presented work for varying 70% of TP for (a) Positive and (b) Negative measures*

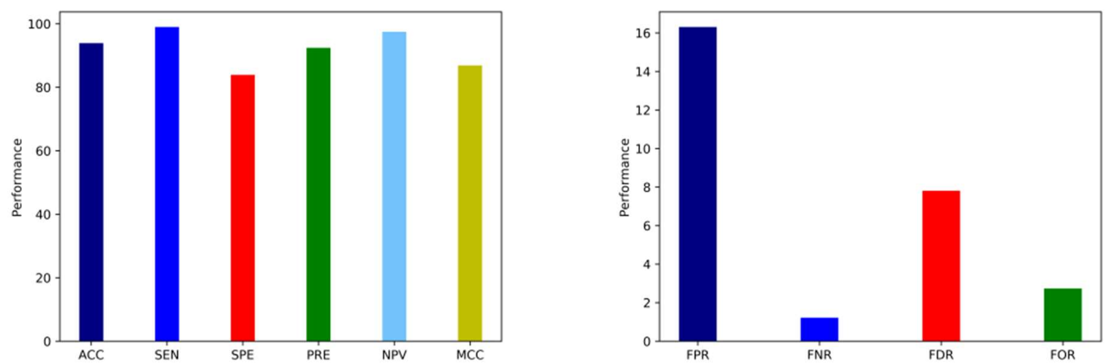

(a) (b)

Fig. 8. *Performance Evaluation of the presented work for varying 80% of TP for (a) Positive and (b) Negative measures*

6.3 Overall Performance Evaluation of Presented Work

The overall performance of the presented model (SC-ROA+GA+ADAM) is evaluated over the traditional models to exhibit its superiority. This evaluation is undergone at TP=70 and the resultants acquired are shown graphically in Fig.9 . The accuracy of the presented work (~91.74) is higher than the existing works and it is 2.5%, 6%, 2.2%, and 1.9% better than the conventional optimizers like SGD, ADAGRAD, RMSPROP, and ADAM in Fig. 9(a). Further, in Fig. 9(b), the sensitivity of the presented work (~96.63) is higher, while compared to the other existing works SGD (~99.44), ADAGRAD (~96.428), RMSPROP (~95.40) and ADAM (~95.40). Thus, the sensitivity of the presented works is 4.6%, 12.6%, 3.8%, and 3% better than SGD, ADAGRAD, RMSPROP, and ADAM, respectively. The other positive measures like specificity (in Fig. 9(c)) and precision (in Fig. 9(d)) also exhibit higher resultants for the presented work, when compared to the extant ones. The negative performance measures of the presented work over the existing one are exhibited in Fig. 10. The FPR of the presented work (~10) in Fig. 10(a), is the lowest one and it is 83%, 53.27%, 25.5%, and 21.3% better than the traditional approaches like SGD (~18.382), ADAGRAD (~21.428), RMSPROP (~13.44) and ADAM (~12.711), respectively. On the other hand, in Fig. 5(f), the FDR of the presented work (~5.737) is the lowest one and it is 53.4%, 61.98%, 27.1%, and 22.3% better than the existing approaches like SGD, ADAGRAD, RMSPROP, and ADAM, respectively. Thus, from the evaluation, it is clear that the presented work is better than the traditional works.

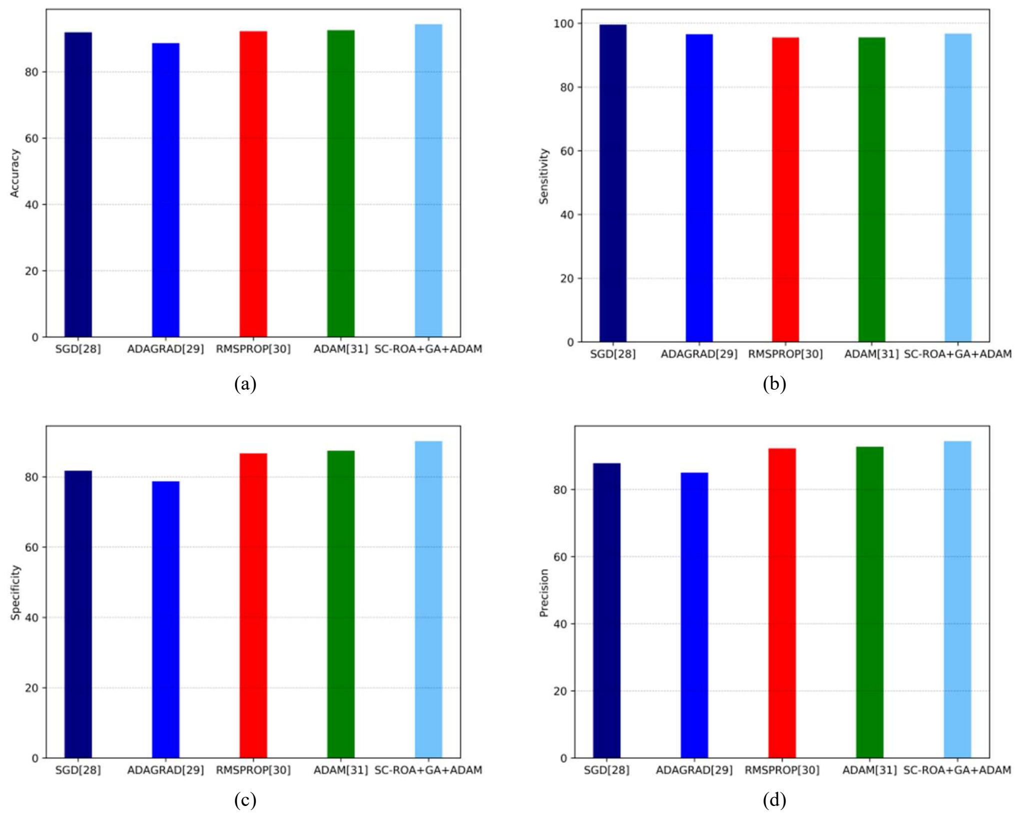

Fig. 9. *Overall positive Performance Evaluation of the presented work over existing works on (a) Accuracy (b)Sensitivity (c) Specificity and (d) Precision*

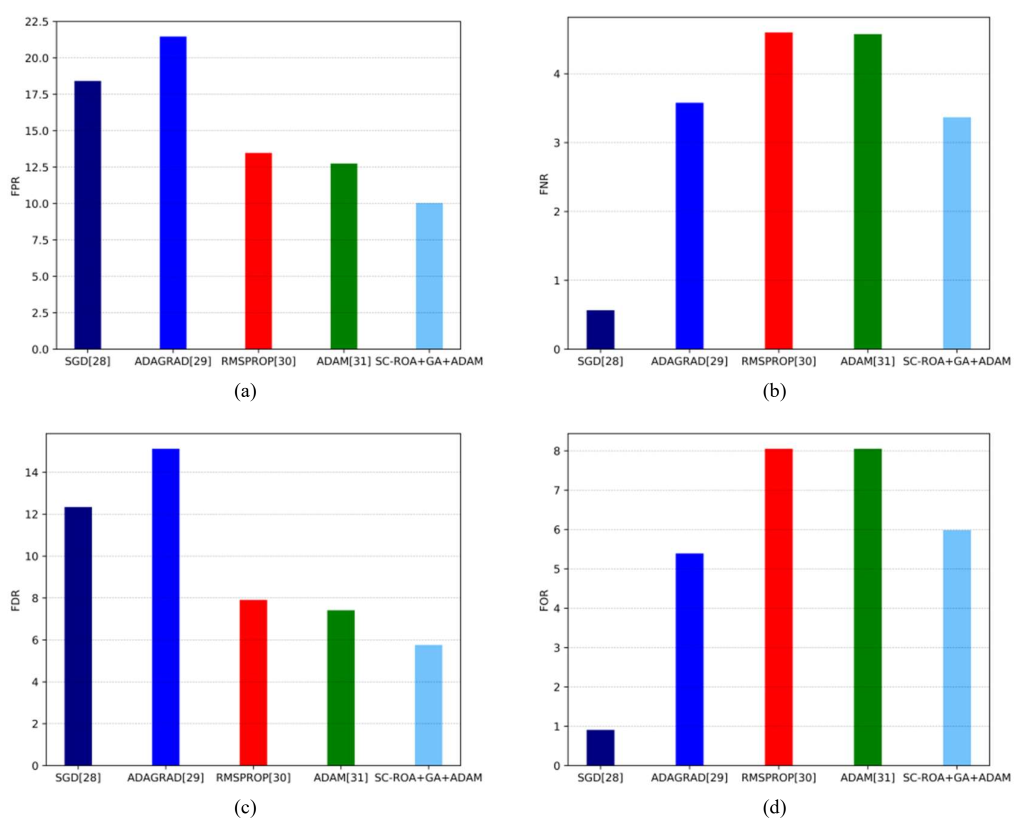

Fig. 10. *Overall Negative Performance Evaluation of the presented work over existing works on (a) FPR (b)FNR (c) FDR and (d) FOR*

6.4 Computing Time Evaluation

The computing time of the presented model (SC-ROA+GA+ADAM) is evaluated over the existing works and the results acquired are tabulated in Table II. From the table, the SGD takes the lowest computing time, while the presented work consumes the highest one. Even though the computing time of the presented work is the highest one, its performance is still much better than the existing works. Future research works might intend to reduce the computing time without affecting the performance.

Table 2: *Analysis of Computing Time*

Methods	Computing Time
SGD	484.7186076641083
ADAGRAD	540.4565615653992
RMSPROP	539.8710386753082
ADAM	1272.0885665416718
SC-ROA+GA+ADAM	31393.83070373535

7. Advantages and Disadvantages

Advantages

1. The proposed method achieves a low false negative rate and false discovery rate, which is beneficial for accurate image retrieval.
2. The method utilizes multi-modal stacked deep probabilistic networks (MM-SDPN) and content-based image retrieval (CBIR) techniques, which can enhance retrieval performance.
3. SVM and 3D-CapsNets are employed in the proposed method, which can improve the classification accuracy and feature representation of the images.
4. The method incorporates clustering via the network (CluViaN) and cumulative distribution function (CDF) to further enhance the retrieval performance.
5. The proposed hybrid optimization algorithm provides overall weight results, which can contribute to the success rate evaluation of the search agent.

Disadvantages

It often requires significant computational resources and large amounts of labeled data for training. Such datasets can be expensive and time-consuming.

8. Conclusion

This paper developed a novel Alzheimer's disease detection approach by following two phases namely, (a) pre-processing and (b) classification. The collected were pre-processed using CLAHE and were filtered using Gaussian blur, median blur, and bi-lateral blur. These filtered images were subjected to classification via optimized CNN, where the outcomes are acquired. As a novelty, the weight of optimized CNN was regularized via a new SC-ROA approach and these regularized weights were optimized with GA and ADAM optimizers. The final optimized weights were acquired from GA and the objective function is texted and evaluated here. Finally, the presented work was compared with the existing works to reveal its supremacy. The accuracy of the presented work (~91.74) is higher than the existing works and it is 2.5%, 6%, 2.2%, and 1.9% better than the conventional optimizers like SGD, ADAGRAD, RMSPROP, and ADAM. Investigating the potential application of the proposed method in other domains or medical imaging datasets could provide insights into its versatility and effectiveness. The integration of additional modalities or features could be explored to enhance the accuracy and robustness of the content-based image retrieval (CBIR) system.

Compliance with Ethical Standards

Conflicts of interest: Authors declared that they have no conflict of interest.

Human participants: The conducted research follows the ethical standards and the authors ensured that they have not conducted any studies with human participants or animals.

References

[1] M. Rahim, B. Thirion, C. Comtat, and G. Varoquaux, "Transmodal Learning of Functional Networks for Alzheimer's Disease Prediction," in IEEE Journal of Selected Topics in Signal Processing, vol. 10, no. 7, pp. 1204-1213, Oct. 2016.

[2] J. Shi, X. Zheng, Y. Li, Q. Zhang, and S. Ying, "Multimodal Neuroimaging Feature Learning With Multimodal Stacked Deep Polynomial Networks for Diagnosis of Alzheimer's Disease," in IEEE Journal of Biomedical and Health Informatics, vol. 22, no. 1, pp. 173-183, Jan. 2018.

[3] K. R. Kruthika, Rajeswari, H. D. Maheshappa, Alzheimer's Disease Neuroimaging Initiative, "Multistage classifier-based approach for Alzheimer's disease prediction and retrieval", Informatics in Medicine, vol.14, pp.34-42, 2019.

[4] Ruoxuan Cui, Manhua Liu, "RNN-based longitudinal analysis for diagnosis of Alzheimer's disease", Computerized Medical Imaging and Graphics, vol.73, pp. 1-10, April 2019.

[5] K. R. Kruthika, Rajeswari, H. D. Maheshappa, "CBIR system using Capsule Networks and 3D CNN for Alzheimer's disease diagnosis", Informatics in Medicine Unlocked, vol.14, pp. 59-68, 2019.

[6] Iman Beheshti, Hasan Demirel, Hiroshi Matsuda, "Classification of Alzheimer's disease and prediction of mild cognitive impairment-to-Alzheimer's conversion from structural magnetic resource imaging using feature ranking and a genetic algorithm", Computers in Biology and Medicine, vol.83, pp. 109-119, April 2017.

[7] K. Liu, H. Wang, S. Risacher, A. Saykin, and L. Shen, "Multiple incomplete views clustering via non-negative matrix factorization with its application in Alzheimer's disease analysis," 2018 IEEE 15th International Symposium on Biomedical Imaging (ISBI 2018), Washington, DC, pp. 1402-1405, 2018.

[8] Hazel Nicolette Manners, Swarup Roy, Jugal K. Kalita, "Intrinsic-overlapping co-expression module detection with application to Alzheimer's Disease", Computational Biology and Chemistry, vol.77, pp 373-389, December 2018.

[9] P. Padilla, M. Lopez, J. M. Gorriz, J. Ramirez, D. Salas-Gonzalez and I. Alvarez, "NMF-SVM Based CAD Tool Applied to Functional Brain Images for the Diagnosis of Alzheimer's Disease," in IEEE Transactions on Medical Imaging, vol. 31, no. 2, pp. 207-216, Feb. 2012.

[10] Q. Zhou *et al*., "An Optimal Decisional Space for the Classification of Alzheimer's Disease and Mild Cognitive Impairment," in IEEE Transactions on Biomedical Engineering, vol. 61, no. 8, pp. 2245-2253, Aug. 2014.

[11] X. Wu *et al*., "The Receiver Operational Characteristic for Binary Classification with Multiple Indices and Its Application to the Neuroimaging Study of Alzheimer's Disease," in IEEE/ACM Transactions on Computational Biology and Bioinformatics, vol. 10, no. 1, pp. 173-180, Jan.-Feb. 2013.

[12] Zhenghui Hu and Pengcheng Shi, "Regularity and Complexity of Human Electroencephalogram Dynamics: Applications to Diagnosis of Alzheimer's Disease," 18th International Conference on Pattern Recognition (ICPR'06), Hong Kong, 2006, pp. 245-248.

[13] J. Tung, H. Snyder, J. Hoey, A. Mihailidis, M. Carrillo and J. Favela, "Everyday Patient-Care Technologies for Alzheimer's Disease," in IEEE Pervasive Computing, vol. 12, no. 4, pp. 80-83, Oct.-Dec. 2013.

[14] Y. Hsu *et al*., "Gait and Balance Analysis for Patients With Alzheimer's Disease Using an Inertial-Sensor-Based Wearable Instrument," in IEEE Journal of Biomedical and Health Informatics, vol. 18, no. 6, pp. 1822-1830, Nov. 2014.

[15] J. Wan *et al*., "Identifying the Neuroanatomical Basis of Cognitive Impairment in Alzheimer's Disease by Correlation- and Nonlinearity-Aware Sparse Bayesian Learning," in IEEE Transactions on Medical Imaging, vol. 33, no. 7, pp. 1475-1487, July 2014.

[16] R. Hornero, J. Escudero, A. FernÁndez, J. Poza and C. GÓmez, "Spectral and Nonlinear Analyses of MEG Background Activity in Patients With Alzheimer's Disease," in IEEE Transactions on Biomedical Engineering, vol. 55, no. 6, pp. 1658-1665, June 2008.

[17] Ann D. Cohen, William E. Klunk, "Early detection of Alzheimer's disease using PiB and FDG PET", Neurobiology of Disease, vol.72, pp.117-122, December 2014.

[18] Leonardo Guzmán-Martínez, Gonzalo A. Farías, Ricardo B. Maccioni,"Emerging Noninvasive Biomarkers for Early Detection of Alzheimer's Disease",Archives of Medical Research, Vol.43,no.4,pp.663-666, November 2012.

[19] Stefan Teipel, Alexander Drzezga, Michel J Grothe, Henryk Barthel, Andreas Fellgiebel, "Multimodal imaging in Alzheimer's disease: validity and usefulness for early detection", The Lancet Neurology, Vol.14, no.10, pp.1037-1053, October 2015.

[20] Joseph C. McBride, Xiaopeng Zhao, Nancy B. Munro, Gregory A. Jicha, Yang Jiang, "Sugihara causality analysis of scalp EEG for detection of early Alzheimer's disease", NeuroImage: Clinical, Vol.7, pp.258-265, 2015.

[21] I. Beheshti, H. Demirel, for the Alzheimer's Disease Neuroimaging Initiative, "Probability distribution function-based classification of structural MRI for the detection of Alzheimer's disease", Computers in Biology and Medicine, Vol.64, pp.208-216, September 2015.

[22] Lisa Mosconi, Miroslaw Brys, Lidia Glodzik-Sobanska, Susan De Santi, Mony J. de Leon, "Early detection of Alzheimer's disease using neuroimaging", Experimental Gerontology, Vol.42,pp129-138, February 2007.

[23] M. Ammar, C. Smadja, L. Giang Thi Phuong, M. Azzouz, E. Dufour-Gergam, "A new controlled concept of immune-sensing platform for specific detection of Alzheimer's biomarkers", Biosensors and Bioelectronics, Vol.40, pp.329-335, February 2013.

[24] Cyndy B. Cordell, Soo Borson, Malaz Boustani, Joshua Chodosh, Medicare Detection of Cognitive Impairment Workgroup, "Alzheimer's Association recommendations for operationalizing the detection of cognitive impairment during the Medicare Annual Wellness Visit in a primary care setting", Alzheimer's & Dementia, Vol.9, pp.141-150, March 2013.

[25] Darya Chyzhyk, Manuel Graña, Alexandre Savio, Josu Maiora, "Hybrid dendritic computing with kernel-LICA applied to Alzheimer's disease detection in MRI", Neurocomputing, Vol.75, no.1, pp. 72-77, January 2012.

[26] Binu and Kariyappa," RideNN: A New Rider Optimization Algorithm-Based Neural Network for Fault Diagnosis in Analog Circuits", IEEE Transactions On Instrumentation And Measurement, pp.1-25, May 2018.

[27] S. He, Q. H. Wu, and J. R. Saunders, "Group Search Optimizer: An Optimization Algorithm Inspired by Animal Searching Behavior," in IEEE Transactions on Evolutionary Computation, vol. 13, no. 5, pp. 973-990, Oct. 2009.

[28] Arnulf Jentzen, Philippe von Wurstemberger, "Lower error bounds for the stochastic gradient descent optimization algorithm: Sharp convergence rates for slowly and fast decaying learning rates", Journal of Complexity, vol.57, April 2020.

[29] [A. T. Hadgu, A. Nigam and E. Diaz-Aviles, "Large-scale learning with AdaGrad on Spark," 2015 IEEE International Conference on Big Data (Big Data), Santa Clara, CA, pp. 2828-2830, 2015.

[30] F. Zou, L. Shen, Z. Jie, W. Zhang, and W. Liu, "A Sufficient Condition for Convergences of Adam and RMSProp," 2019 IEEE/CVF Conference on Computer Vision and Pattern Recognition (CVPR), Long Beach, CA, USA, pp. 11119-11127, 2019.

[31] Z. Zhang, "Improved Adam Optimizer for Deep Neural Networks," 2018 IEEE/ACM 26th International Symposium on Quality of Service (IWQoS), Banff, AB, Canada, pp. 1-2, 2018.

[32] M. Marsaline Beno, Valarmathi I. R, Swamy S. M, and B. R. Rajakumar, "Threshold prediction for segmenting tumor from brain MRI scans", International Journal of Imaging Systems and Technology, Vol. 24, No. 2, pages 129-137, 2014.

[33] Elgammal, Y.M., Zahran, M.A. and Abdelsalam, M.M., "A new strategy for the early detection of alzheimer disease stages using multifractal geometry analysis based on K-Nearest Neighbor algorithm", Scientific Reports, Vol. 12(1), pp.22381, 2022.